# Exosomal miRNAs from neutrophils act as accurate biomarkers for gastric cancer diagnosis

Yu, Dan; Zhang, Jiahui; Wang, Maoye; Ji, Runbi; Qian, Hui; Xu, Wenrong; Zhang, Hongbo; Gu, Jianmei; Zhang, Xu

*Published in:*
Clinica Chimica Acta

*DOI:*
10.1016/j.cca.2024.117773

Published: 01/02/2024

*Document Version*
Final published version

*Document License*
CC BY-NC

Clinica Chimica Acta 554 (2024) 117773

Contents lists available at ScienceDirect

Clinica Chimica Acta

journal homepage: www.elsevier.com/locate/cca

# Exosomal miRNAs from neutrophils act as accurate biomarkers for gastric cancer diagnosis

Dan Yu [a], Jiahui Zhang [a], Maoye Wang [a], Runbi Ji [a], Hui Qian [a], Wenrong Xu [a], Hongbo Zhang [c,d,*], Jianmei Gu [b,*], Xu Zhang [a,*]

[a] Department of Laboratory Medicine, School of Medicine, Jiangsu University, Zhenjiang 212013, China
[b] Departmemt of Clinical Laboratory Medicine, Affiliated Cancer Hospital of Nantong University, 226300 Nantong, China
[c] Pharmaceutical Sciences Laboratory, Abo Akademi University, 20520 Turku, Finland
[d] Turku Bioscience Centre, University of Turku and Abo Akademi University, 20520 Turku, Finland

ARTICLE INFO

*Keywords:*
Neutrophils
Exosomes
miRNA
Gastric cancer
Liquid biopsy

ABSTRACT

*Background:* Gastric cancer (GC) is the third leading cause of cancer-related death worldwide. Sensitive and accurate biomarkers can greatly aid in early diagnosis and favorable prognosis. Neutrophils are the most abundant immune cells in human circulation and play a critical role in tumor progression. Neutrophil-derived exosomes (Neu-Exo) contain abundant bioactive molecules and are critically involved in disease progression.
*Methods:* We proposed a Dynabeads-based (CD66b antibody-coupled) separation and detection system for Neu-Exo analysis. Dual antibody-assisted fluorescent Dynabeads was established to detect Neu-Exo abundance. MiRNA signature of Neu-Exo was identified by RNA sequencing. QRT-PCR and droplet digital PCR (ddPCR) were used for candidate miRNA detection and the potential of Neu-Exo miRNAs in the diagnosis of gastric cancer was evaluated.
*Results:* Dual antibody-assisted fluorescent Dynabeads obtained a detection limit of $7.8 \times 10^5$ particles/mL of Neu-Exo and a recovery rate of 81 % under optimized conditions. ROC curve indicated that the abundance of $CD66b^+$ Neu-Exo could well distinguish GC patients from healthy controls (HC) (AUC > 0.8). Additionally, miR-223-3p was found among the top differentially expressed miRNAs in Neu-Exo and presented superior diagnostic value in gastric cancer. Droplet digital PCR (ddPCR) significantly improved the diagnostic efficiency to differentiate GC patients from HC and benign gastric diseases (BGD) patients (AUC > 0.9).
*Conclusion:* The Dynabeads-based separation and detection system, assisted with ddPCR analysis, provides a promising platform to enrich Neu-Exo and analyze miRNA profile for gastric cancer liquid biopsy.

## 1. Introduction

Gastric cancer is one of the most common causes of cancer-related death [1]. Traditional approaches for cancer diagnosis such as tissue biopsy and serology biomarker detection undergo the challenges of invasive-injury, low sensitivity and specificity. Therefore, it's urgent to develop reliable biomarkers for gastric cancer diagnosis. Exosomes, lipid bi-layer membrane vesicles with a diameter ranging from 40 nm to 160 nm, are secreted by almost all cell types and stably circulate in body fluids [2]. By transporting bioactive molecules such as mRNA [3], miRNA [4] and proteins [5], exosomes are critically involved in tumor progression, metastasis, and drug resistance. Exosomes are now being recognized as an ideal indicator for liquid biopsy and have been used for cancer diagnosis, treatment monitoring and prognosis assessment.

Tumor-associated neutrophils (TANs) play important roles in tumor microenvironment. Increasing studies suggest that TANs have dual roles in regulating tumor progression. Native neutrophils (N1 type) play an antitumor role, while N2 TANs promote tumor proliferation, metastasis, drug resistance and recurrence by releasing proteins [6,7], neutrophil extracellular traps [8] and lipids [9–11]. It has been reported that an elevated number of neutrophils and high circulating neutrophil-to-lymphocyte ratio could predict poor outcomes in many cancers [10,12]. Moreover, a high density of $CD66b^+$ TANs is frequently associated with high-grade tumor and poor survival [13]. Recent studies

* Corresponding authors at: School of Medicine, Jiangsu University, Zhenjiang, Jiangsu 212013, China (X. Zhang). Affiliated Cancer Hospital of Nantong University, Nantong, Jiangsu 226300, China (J. Gu). Abo Akademi University, 20520, Finland (H. Zhang).
*E-mail addresses:* hongbo.zhang@abo.fi (H. Zhang), gujianmei2010@163.com (J. Gu), xuzhang@ujs.edu.cn (X. Zhang).

https://doi.org/10.1016/j.cca.2024.117773
Received 12 June 2023; Received in revised form 10 December 2023; Accepted 7 January 2024
Available online 9 January 2024

highlight that neutrophil-derived exosomes (Neu-Exo) are involved in disease progression. For example, lncRNA CRNDE delivered by LPS-activated Neu-Exo enhances the proliferation and migration of smooth muscle cells and facilitates the airway remodeling in asthma [14]. Exosomal miR-4466 from nicotine-activated N2 neutrophils promotes tumor cell stemness and metastasis. The elevated expression of exosomal miR-4466 is found in the serum/urine of cancer-free subjects with smoking history, which indicates the potential of miR-4466 as a prognostic biomarker to predict the increased risk of metastatic diseases among smokers [15]. Moreover, Neu-Exo-derived SPI1 mRNA is delivered to colon cancer cells, which activates the downstream glycolytic genes and promotes the glycolysis and metastasis of tumor cells. The up-regulation of SPI1 mRNA indicates poor prognosis in patients with colon cancer [16]. Therefore, Neu-Exo participate in the process of tumor development and progression and may serve as a potential biomarker for cancer diagnosis and prognosis.

The use of exosomes as biomarkers is severely constrained by the technical difficulties in isolation and molecular detection. Although novel technologies such as size-exclusion chromatography [17], microfluidic chip [18] and thermophoresis [19] have been developed, ultracentrifugation is still the accepted gold standard for exosome separation. Traditional exosome detection techniques, such as PCR, western blot, and ELISA, require lengthy processes and substantial sample volumes, which greatly limits the clinical practical use. Therefore, novel exosome biomarkers combined with rapid and highly sensitive isolation and detection platform are essential for cancer liquid biopsy.

In this study, we found that Neu-Exo miRNAs may act as accurate biomarkers in gastric cancer diagnosis. We proposed a strategy to separate and analyze Neu-Exo by using CD66b antibody-coupled Dynabeads. Dual antibody-assisted fluorescent Dynabeads was established to detect the abundance of $CD66b^{+}$ Neu-Exo in human serum. The potential of $CD66b^{+}$ Neu-Exo to distinguish GC patients from healthy individuals was evaluated (Fig. 1A, C). RNA sequencing was then conducted to profile the differentially expressed miRNAs in the serum Neu-Exo of GC patients. MiR-223-3p was found with high diagnostic value to identify GC of different stages. In addition, ddPCR was applied for miRNA detection, which significantly improved the diagnostic efficiency (Fig. 1B, C). These results suggest that the detection of Neu-Exo miRNAs may provide an effective tool for the early diagnosis of gastric cancer.

## 2. Materials and methods

### 2.1. Experimental reagents

Dynabeads® antibody coupling kit, 4 μm aldehyde/sulfate latex beads and Dio cell-labeling solutions were bought from Invitrogen (USA). Bovine serum albumin (BSA) was purchased from Biofroxx (German). FITC mouse anti-human CD66b antibody (G10F5) and FITC mouse IgM isotype control antibody (MM-30) were bought from Biolegend (USA). Fetal bovine serum (FBS) and RPMI 1640 were acquired from Gibco (USA). MiRNeasy Serum/Plasma Kit was obtained from QIAGEN (German). BCA protein assay kit was acquired from Vazyme (China). Primers and miRNA qRT-PCR Starter Kit were purchased from RuiBo Company (China). Sapphire Chips for Naica Crystal ddPCR system was purchased from STILLA technologies (France).

### 2.2. Isolation of exosomes from cell culture medium by ultracentrifugation

Neutrophils were isolated from the peripheral blood of healthy volunteers by using polymorphprep (Axis-Shield Po CAS, Norway) and identified by Reye's staining. To evaluate the CD66b expression of neutrophils, $1 \times 10^5$ cells were incubated with 1 μL FITC-labeled mouse anti-human CD66b antibody in 100 μL PBS (phosphate buffered saline) at 4 °C for 30 min. FITC mouse IgM-stained cells were set as the isotype control. After washing with PBS twice, the cells were subjected to flow cytometry analysis (Fig. 2A).

Neutrophils were cultured in RPMI 1640 containing 10 % of exosome-free FBS at the conditions of 5 % $CO_2$ and 37 °C, and the cell culture medium was collected for 24 h. The culture medium of neutrophils was sequentially centrifuged at 300 g for 20 min, 2000 g for 20

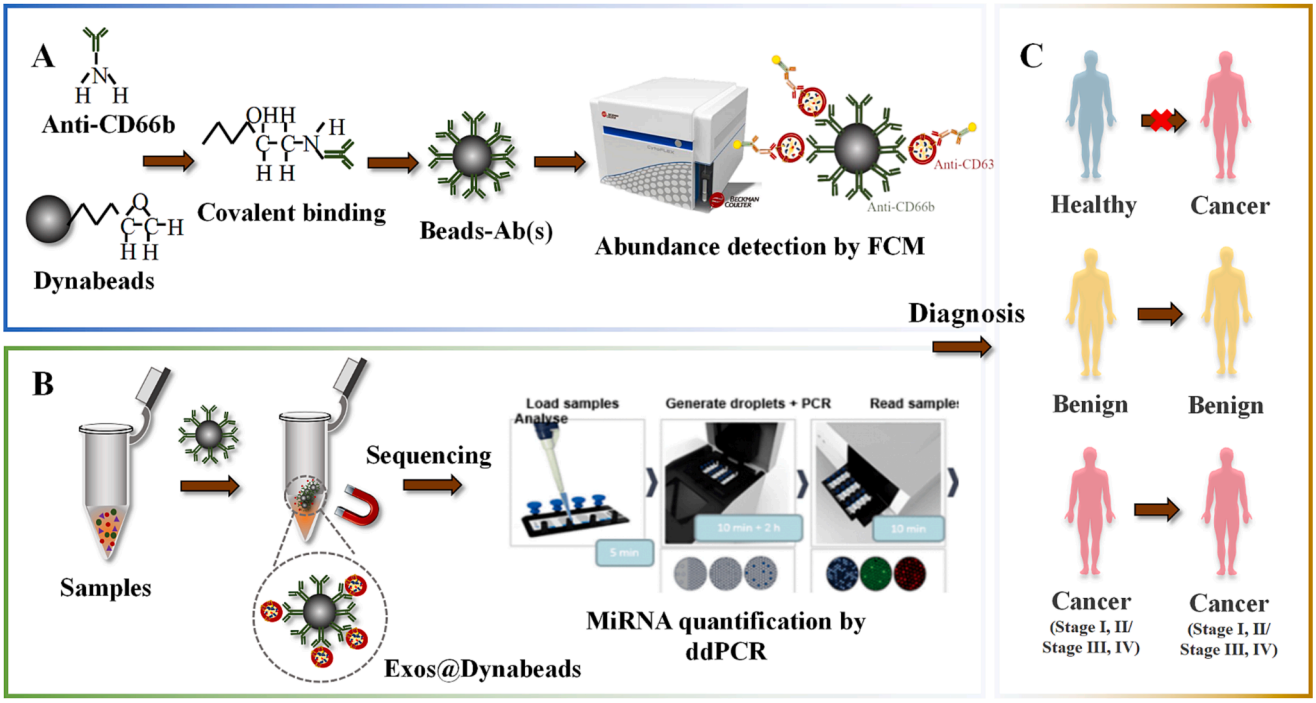


**Fig. 1.** Schematic diagram of Dynabeads-based Neu-Exo separation and detection system. (A) Fabrication of CD66b antibody-coupled Dynabeads for Neu-Exo capture and abundance detection. (B) Neu-Exo separation and RNA Sequencing, followed by candidate miRNA screening and ddPCR detection. (C) Evaluation of the diagnostic efficiency of Neu-Exo and their derived miRNAs in differentiating healthy control, benign gastric disease, and gastric cancer groups.

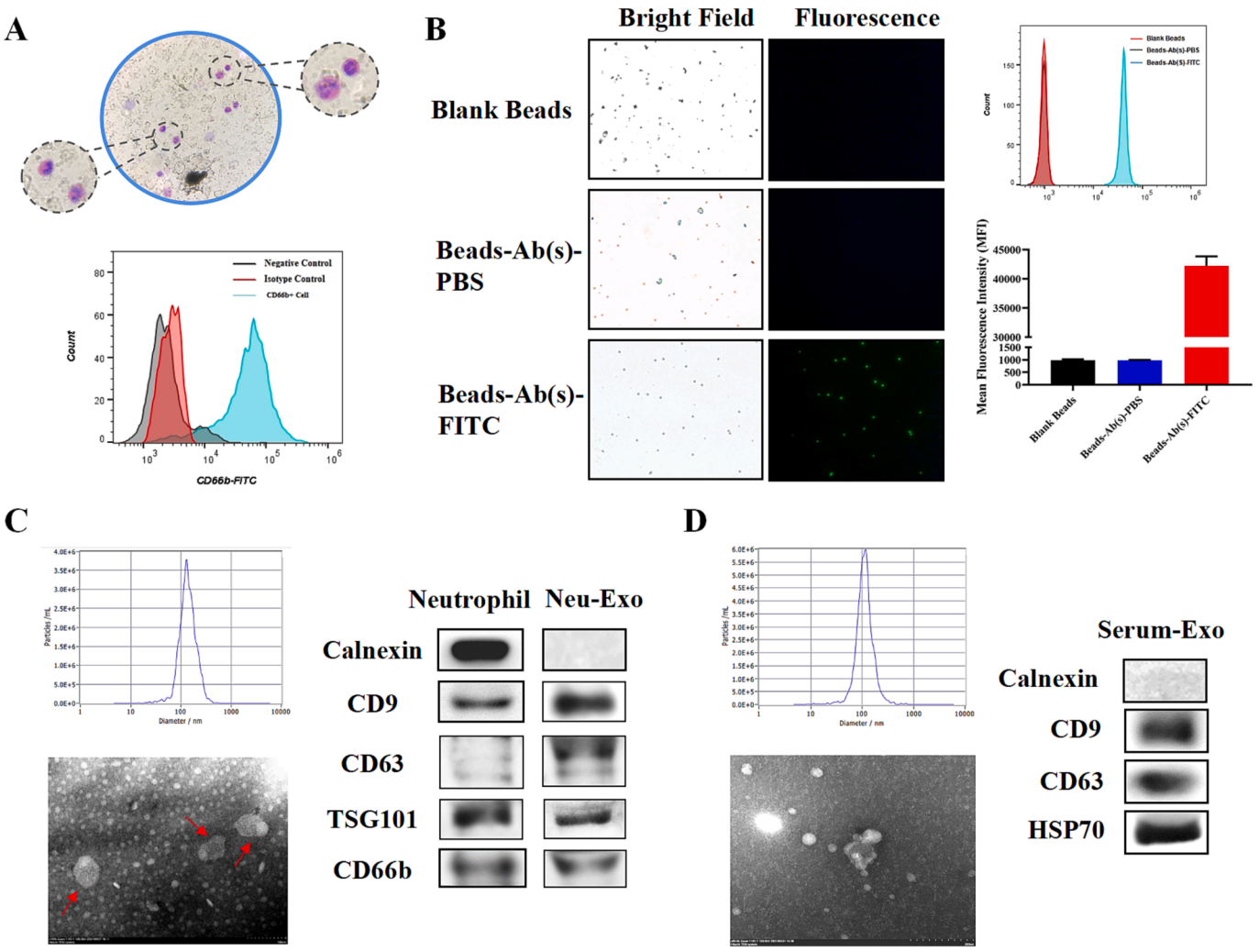


**Fig. 2.** Identification and characterization of neutrophils, antibody-coupled Dynabeads and exosomes. (A) Neutrophil identification by Reye's staining and flow cytometry. (B) Characterization of CD66b antibody-coupled Dynabeads by fluorescence microscope. (C-D) Characterization of (C) Neu-Exo and (D) Serum-Exo by NTA, TEM and western blot.

min, and 10,000 g for 30 min, and then filtered through 0.22 μm Millex-GV filter (Merck Millipore) to remove cells, cell debris and large extracellular vesicles. The final supernatants were centrifuged by ultracentrifugation at 100,000 g for 70 min twice, and the exosome pellets were re-suspended with 500 μL PBS and stored at --80 °C until use.

### 2.3. Sample collection and exosome isolation by ultracentrifugation

Serum samples of GC patients, benign gastric disease (BGD) patients and healthy controls (HC) were collected from the Affiliated People's Hospital of Jiangsu University. Informed consent was obtained from all the subjects in this study. The inclusion criteria were as follows: (1) histologically confirmed gastric cancer; (2) primarily diagnosed GC without surgical treatment, radiotherapy or chemotherapy; (3) clinicopathological information is available for collection. The patients with multiple primary cancers and incomplete clinicopathological data were excluded. The study was performed in accordance with the clinical study protocol approved by the Institutional Review Board and approved by the Medical Ethics Committee of Jiangsu University.

The collected serum samples (500 μL) were first centrifuged at 12,000g for 20 min at 4 °C and then filtered through 0.22 μm filters. After diluting to 40 mL by PBS, the supernatants were ultracentrifuged at 100,000g, 4 °C for 2 h, and the exosome pellets were re-suspended in 500 μL PBS and stored at --80 °C.

### 2.4. Preparation of CD66b antibody-coupled Dynabeads

Due to the high specificity of cell origin and close association with gastric cancer prognosis [20], CD66b was selected as the exosomal membrane protein marker for Neu-Exo separation. Following the manufacturer's instructions, the CD66b capture beads were generated by coupling 12 μg CD66b antibody (Abcam, ab197678) to 2 mg Dynabeads (2.8 μm in diameter) through the covalently binding of epoxy groups on the surface of beads and the primary amino groups in antibodies. The coupling reaction was performed at 37 °C for at least 18 h with gentle shaking. After removing supernatant by magnetic separator (Merck Millipore), the retained Dynabeads were resuspended in 200 μL Storage Buffer for further use.

### 2.5. Separation of Neu-Exo by CD66b antibody-coupled Dynabeads

To separate Neu-Exo, total exosomes isolated by ultracentrifugation from culture medium or human serum were mixed with prepared CD66b antibody-coupled Dynabeads. The mixture was then diluted to 400 μL with PBS and left at 4 °C with continuous rotation. To verify the best reaction condition, exosomes from the culture medium of neutrophils were considered as model samples. Different volumes of Dynabeads suspension (2 μL to 6 μL) were gently mixed with the same amounts of exosomes at 4 °C. The certain amounts of beads and exosomes were

incubated for different times. Exosomes captured by beads (Exos@Dynabeads) were separated by external magnet and subjected for BCA analysis. The capture efficiency was calculated as the ratio of protein concentration of captured Neu-Exo to that of original exosomes. Additionally, the captured Neu-Exo were eluted with 200 μL of glycine-HCl buffer (pH 2.8) and washed two times with PBS by Amicon Ultra-15 mL (Millipore, US) to obtain the suspension of Neu-Exo.

### 2.6. Characterization of exosomes and Exos@Dynabeads

Exosomes were characterized by western blot, nanoparticle tracking analysis (NTA) and transmission electron microscope (TEM) (Fig. 2C, D). The expression of exosomal CD63 (Abcam, KILL150A), CD9 (CST, P21926), HSP70 (CST, P0DMV8), CD66b (Abcam, EPR25354-2) and negative control calnexin (Abcam, ab75801) were detected by western blot. Exosome samples (diluted in 1 mL PBS) were injected into the chamber for size distribution measurement by NanoSight LM10 system (NTA, UK). The morphologies of exosomes and Exos@Dynabeads were characterized by TEM. The samples were suspended in 20 μL PBS and loaded on copper grids for 5 min fixation. Next, 2 % phosphotungstic acid (PTA) was added to stain for another 5 min. After washing with PBS, the samples were dried at room temperature for observation.

### 2.7. Immunofluorescence

Exosomes were fixed on the poly-L-lysine coated slides at room temperature for 30 min and incubated with the primary antibodies against CD66b (1:50, rabbit anti-human, Abcam, ab197678) and CD63 (1:50, mouse anti-human, Abcam, KILL150A) at 4 °C overnight. The slides were washed with PBS twice to remove the unbound antibodies, followed by incubation with Cy3-labeled secondary antibody (rabbit) and FITC-labeled secondary antibody (mouse) for 1 h. After three times of washing with PBS, the slides were blocked with neutral resin and examined under laser confocal fluorescence microscope.

### 2.8. Detection of $CD66b^+$ Neu-Exo by flow cytometry (FCM)

A method based on dual antibody-assisted fluorescent Dynabeads combined with flow cytometry analysis was developed to detect the abundance of Neu-Exo. CD66b antibody-coupled Dynabeads was applied for exosome capturing. Anti-CD63 antibody, serving as detective antibody, was incubated with Exos@Dynabeads suspension (1 μL antibody in 25 μL of 2 % BSA/PBS) for 1 h at room temperature. After two times of washing, Exos@Dynabeads were incubated with FITC-labeled anti-CD63 secondary antibodies (1 μL antibody in 100 μL of 2 % BSA/PBS) for 2 h with rotation. Secondary antibody alone was set as control. Exos@Dynabeads were finally resuspended in 400 μL PBS for FCM analysis, and the percent of positive beads relative to the total beads analyzed was defined as the percentage of $CD66b^+$ Neu-Exo. For further verification, we conducted CD63 antibody-coated Dynabeads for exosome capturing, and detected with FITC-labeled CD66b antibody. The same procedure was conducted by flow cytometry.

### 2.9. MiRNA sequencing and quantification

Neu-Exo separated from serum of gastric cancer patients and healthy individuals were subjected for miRNA library construction and sequencing by Shanghai Biotechnology Corporation. The RNA of Neu-Exo was extracted by MiRNeasy Serum/Plasma Kit, and the purity was verified by NanoDrop2000 (Thermo Scientific). The total RNA was reverse transcribed to cDNA via miRNA qRT-PCR Starter Kit and the expression level of candidate miRNA was quantified by qRT-PCR.

The ddPCR reaction system contains 1 μM of primers, 3.75 μL of PerfeCTa MultiPlex qPCR Tough Mix, 2 μL of Evagreen, 1 μL of Alexa Fluor 647, 12.75 μL of Nuclease-free water and 5 μL of cDNA products. The reaction mix was then loaded into the inlets of Sapphire chip and incubated at 95 °C for 10 min, followed by 40 cycles at 95 °C for 2 s, 60 °C for 20 s and 70 °C for 10 s. Finally, the chip was subjected for reading in the Crystal Reader software. The recombinant plasmids encoding miR-223-3p and U6 genes were synthesized by Sangon Biotech (Shanghai) and served as standards for analytical performance evaluation.

## 3. Results

### 3.1. Characterization and optimization of exosome capture

To evaluate the successful conjugation of CD66b antibody, we used FITC-labeled goat anti-rabbit secondary antibody to specifically interact with primary antibody on the surface of Dynabeads. Significantly enhanced green fluorescence was observed from secondary antibody-modified beads, which demonstrated that CD66b primary antibody was successfully decorated (Fig. 2B). For the characterization of exosome capturing, model exosome samples were labeled with Dio fluorescence dye. As shown in Fig. 3A, the Dio-labeled exosomes were found captured by Dynabeads due to the specific immune interaction. TEM images showed that typical cup-shaped exosomes were attached to the surface of beads (Fig. 3B). After elution by glycine-HCl, the recovered exosomes could be clearly viewed by TEM (Fig. 3A, C). NTA results displayed a unimodal size distribution of recovered exosomes at 160 nm, which was similar in size to original model exosomes (Fig. 3D). Western blot showed the high expression of exosomal markers (CD9, CD63, HSP70) and neutrophil-specific marker (CD66b), while no expression of calnexin (Fig. 3E). These results suggested that the CD66b antibody-coupled Dynabeads achieved the enrichment of Neu-Exo with a high-purity. Moreover, the process of capture and elution did not affect the morphology and particle size of exosomes.

For the maximum capture efficiency, we optimized the volume of beads and incubation time. Fig. 4A indicated that the amounts of captured exosomes were directly proportional to beads volume, and tended to reach saturation at 5 μL of beads. Incubation time is an important factor for sufficient and effective exosome capturing. We found that 12 h was the optimized duration (Fig. 4B). Consequently, the proposed antibody-modified Dynabeads achieved a capture efficiency of 81 % under optimized conditions (Fig. 4C).

### 3.2. Performance evaluation of the dual antibody-assisted fluorescent Dynabeads

Dual antibody-assisted fluorescent Dynabeads were established based on the colocalization of CD66b and CD63 protein on the membrane of Neu-Exo (Fig. 5A). Model exosome samples were diluted to various concentrations to investigate the sensitivity of fluorescent Dynabeads. As presented in Fig. 5B, the relative fluorescence intensity (RFI) increased linearly with exosome concentration ranging from $1.1 \times 10^6$ to $1.1 \times 10^{11}$ particles/mL with a detection limit of $7.8 \times 10^5$ particles/mL, which has a relatively high sensitivity for further analysis [21,22]. Lymphocyte-derived exosomes (Lym-Exo), with no expression of CD66b, were set as negative control for specificity evaluation. Lymphocytes and Lym-Exo were characterized by FCM and western blot (Figure S1 A, B). As demonstrated in Fig. 5C, CD66b positive beads accounted for 70 % of the total beads analyzed for Neu-Exo, while almost none of the beads were detected positively in Lym-Exo. In addition, the RFI of Neu-Exo showed approximately 6 folds higher than that of Lym-Exo. These results indicate that the dual antibody-assisted fluorescent Dynabeads enabled specific recognition and sensitive detection of Neu-Exo.

### 3.3. Examination of clinical samples

The differential percentage of $CD66b^+$ Neu-Exo in the serum of GC patients and healthy donors was firstly identified by traditional

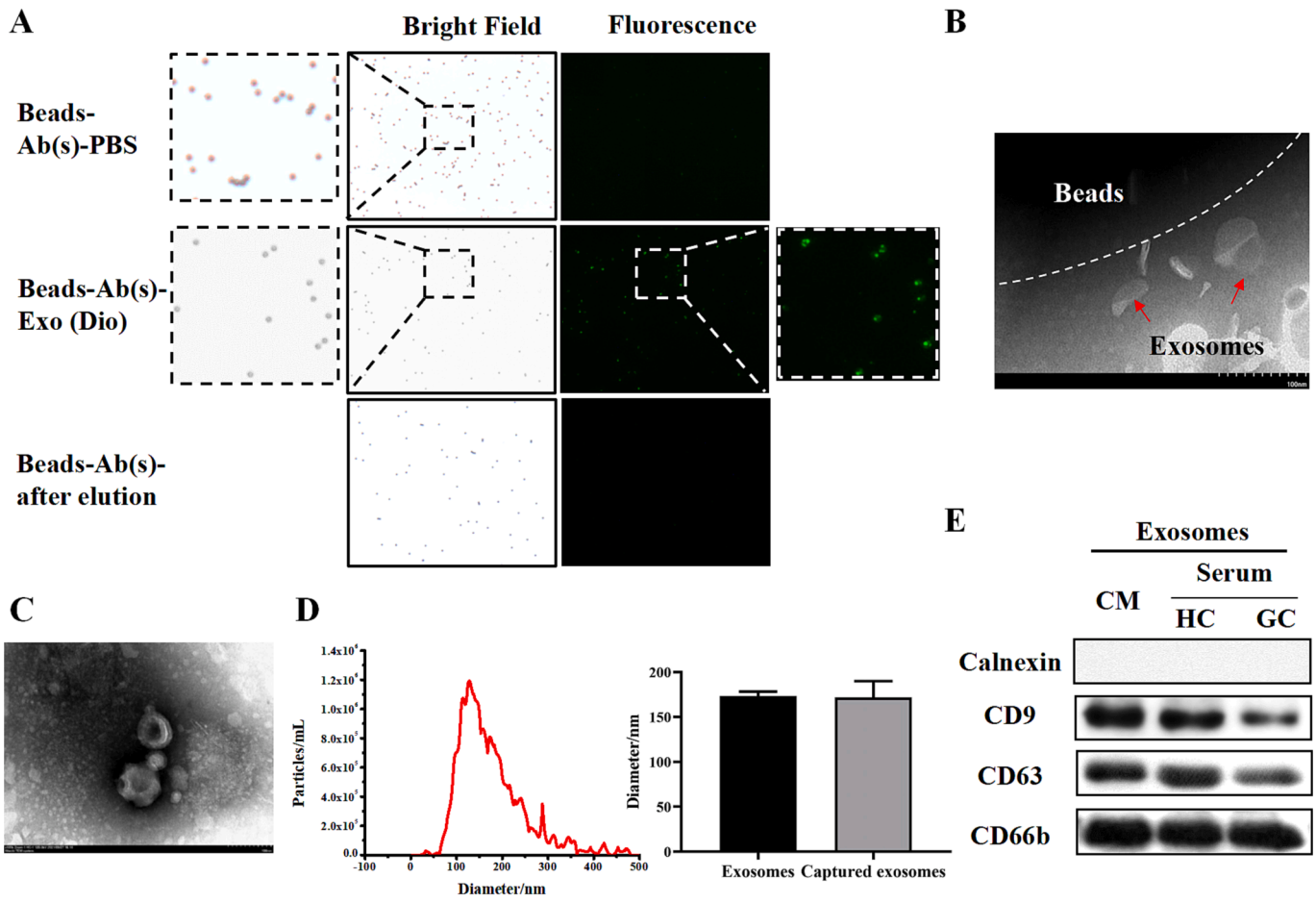


**Fig. 3.** Characterization of exosome capture and recovery. (A) Capturing of Dio-stained model exosomes by Dynabeads under laser confocal fluorescence microscope. (B) Morphology characterization of Exos@Dynabeads (red arrow) by TEM. (C) TEM images of the recovered exosomes. (D) Size distribution of the recovered exosomes. (E) Western blot analysis of exosomal proteins and neutrophil-specific proteins in the recovered exosomes. (For interpretation of the references to colour in this figure legend, the reader is referred to the web version of this article.)

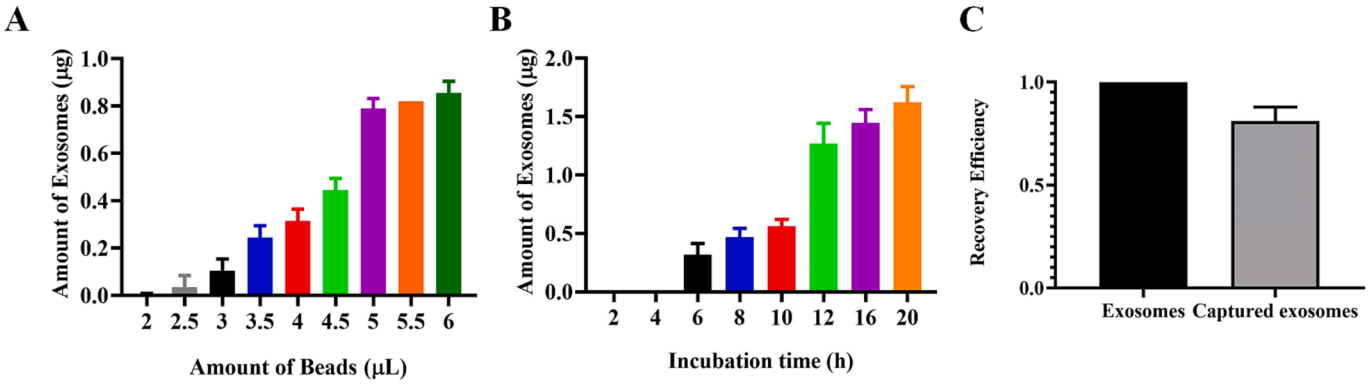


**Fig. 4.** Optimization of dual antibody-assisted fluorescent Dynabeads. (A) Optimization of beads volume. (B) Optimization of incubation time. (C) The recovery efficiency of Dynabeads under optimized conditions.

aldehyde/sulfate latex beads (Figure S1D) [5]. Next, the developed dual antibody-assisted fluorescent Dynabeads were further applied in serum samples. As shown in Figure S1E and F, a higher percentage of CD66b$^+$ Neu-Exo was detected in GC patients compared to healthy controls. NTA results demonstrated significantly increased particle concentration of CD66b$^+$ Neu-Exo in GC patients (Figure S1C). The conclusion was further verified in a larger population containing 27 GC samples and 27 healthy controls (Fig. 5D). ROC curve showed that the area under the curve (AUC) of CD66b$^+$ Neu-Exo to differentiate between GC and HC groups was 0.809 with a sensitivity of 77.78 % and specificity of 74.07 % (Fig. 5E). Therefore, CD66b$^+$ Neu-Exo may be a promising indicator for gastric cancer diagnosis.

### 3.4. *Molecular profiling of Neu-Exo from gastric cancer patients*

MiRNA sequencing was carried out on 6 serum Neu-Exo samples (3 gastric cancer patients and 3 healthy donors). As a result, we obtained 28 up-regulated miRNAs and 5 down-regulated miRNAs (Fig. 6A). To

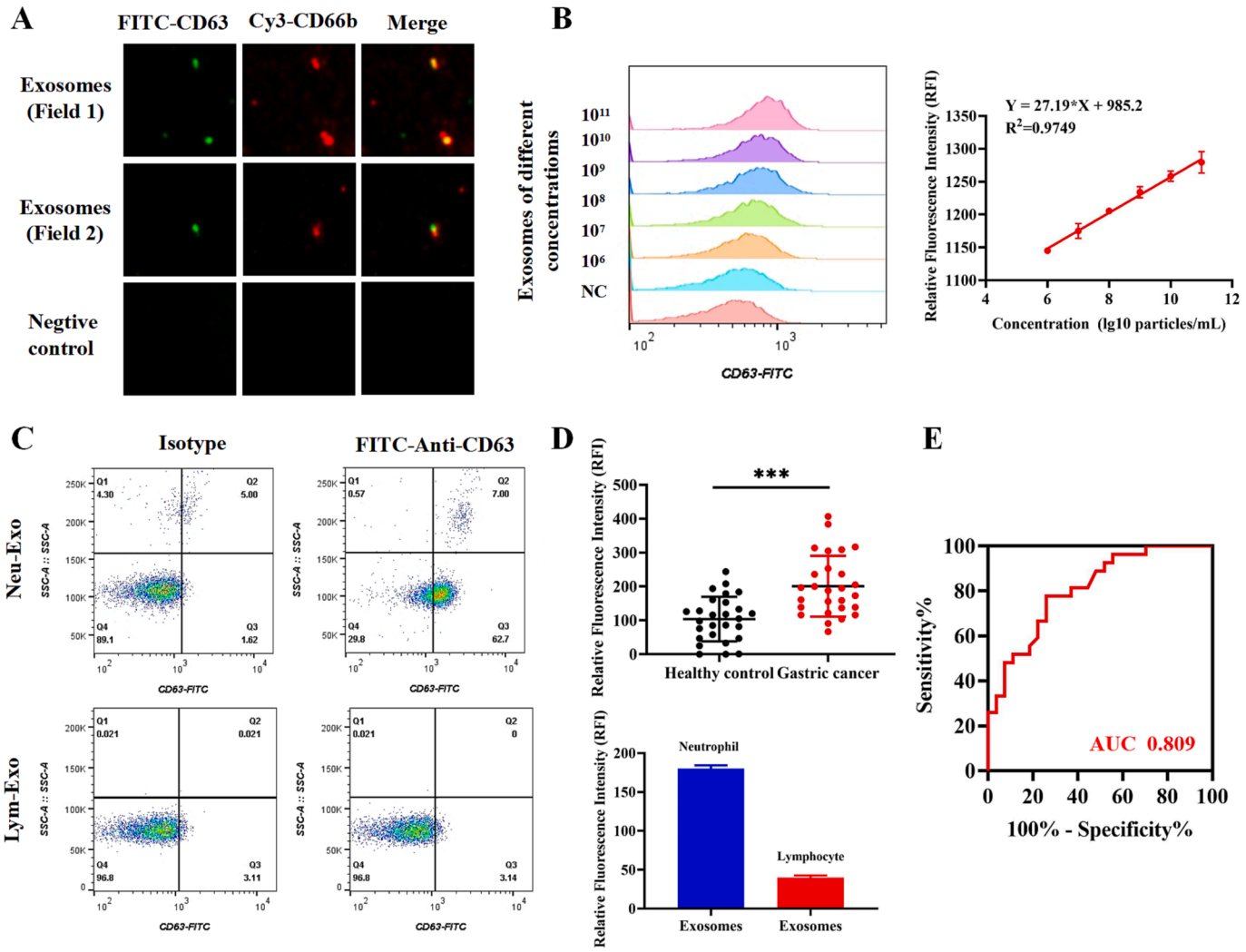


**Fig. 5.** Analytical performance and clinical validation of dual antibody-assisted fluorescent Dynabeads. (A) The colocalization of CD66b and CD63 on the membrane of Neu-Exo observed by laser confocal fluorescence microscope. (B) Linear curve of RFI and model exosomes with gradient concentrations. (C) Specificity assay of fluorescent Dynabeads in detecting Neu-Exo and Lym-Exo by flow cytometry. (D) Detection of $CD66b^{+}$ Neu-Exo in GC patients and healthy controls by fluorescent Dynabeads (***, $P < 0.001$). (E) ROC curve of $CD66b^{+}$ Neu-Exo to distinguish GC patients from healthy individuals.

verify the diagnostic value of miRNAs, the expression of up-regulated miRNAs was detected in neutrophils and Neu-Exo by qRT-PCR (Fig. 6B, C). Finally, two highly expressed miRNAs (miR-223-3p and miR-425-5p) were selected as candidate biomarkers for clinical validation.

### 3.5. MiRNA quantification and diagnostic value evaluation by qRT-PCR

We next evaluated the diagnostic value of candidate miRNAs in serum Neu-Exo of 49 healthy controls, 36 BGD patients and 61 GC patients. As shown in Fig. 6E, miR-223-3p and miR-425-5p were significantly up-regulated in Neu-Exo of GC patients compared to HC and BGD patients. Correlation analysis of clinicopathological features showed that the expression of miR-223-3p in serum Neu-Exo was significantly related to distant metastasis of gastric cancer, while that of miR-425-5p was related to tumor size (Table S1 and S2). ROC curve was used to assess the diagnostic efficiency of single or combined miRNAs analysis. The AUC of miR-223-3p was 0.806 in distinguishing GC patients from healthy controls, while miR-425-5p was 0.744 (Fig. 6F). The combination of miRNAs showed a higher accuracy of 0.847, with 77.05 % of sensitivity and 75.51 % of specificity. In addition, we found that these two miRNAs presented a good differentiation between BGD and GC groups as well (Fig. 6G). Moreover, as illustrated in Fig. 6H, miR-223-3p and miR-425-5p displayed differential expression between non-cancer group (BGD and HC groups) and different stage GC patients. The AUC of combined miRNAs was 0.747 to identify early-stage GC patients (stage I and II), and 0.864 to differentiate late-stage GC patients (stage III and IV) (Fig. 6I, J). Notably, the expression of miR-223-3p in Neu-Exo was found to be significantly higher in gastric cancer patients with distant metastasis than those without metastasis or with lymph node metastasis (Fig. 6D). Furthermore, we compared the diagnostic value of miR-223-3p and miR-425-5p in Neu-Exo and total serum exosomes (Serum-Exo). It was found that the diagnostic efficiency of miRNA in Neu-Exo was significantly superior to that in Serum-Exo (Figure S2A-D, Table S3). Together, these results suggest that miRNAs in serum Neu-Exo are of great significance in the diagnosis of gastric cancer, and the combined biomarkers could increase the diagnostic efficiency.

### 3.6. Optimization and performance evaluation of ddPCR

Droplet digital PCR has the advantage of absolute quantification. We further detected miR-223-3p in serum Neu-Exo by ddPCR to improve the diagnostic efficacy. First, we optimized the primer concentrations in a range of 100–300 nM for better separation. As presented in Fig. 7A, B, relatively concentrated clusters of droplets were achieved under a condition of 250 nM primer for miR-223-3p and 100 nM primer for U6.

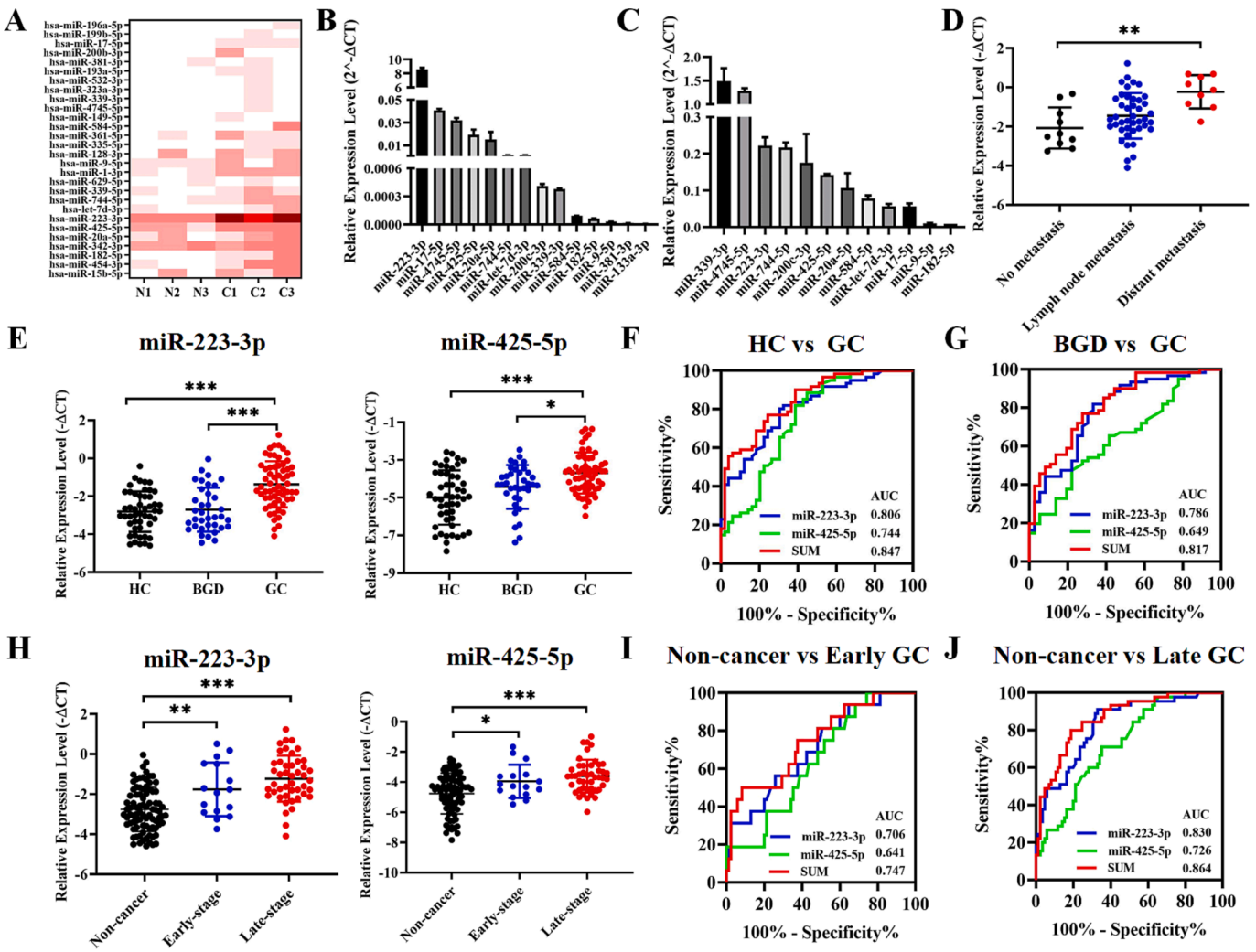


**Fig. 6.** MiRNA sequencing and miRNA detection by qRT-PCR and the diagnostic efficiency in gastric cancer. (A) Differentially expressed miRNA in Neu-Exo obtained by RNA sequencing. (B-C) The detection of up-regulated miRNAs in (B) neutrophils and (C) Neu-Exo. (D) The expression of miR-223-3p was significantly associated with GC distant metastasis. (E) The expression of miR-223-3p and miR-425-5p in HC, BGD and GC groups (***, $P < 0.001$). (F-G) ROC curve of miR-223-3p, miR-425-5p and the combined miRNA in distinguishing between (F) GC patients and healthy controls (G) GC patients and BGD patients. (H) The expression of miR-223-3p and miR-425-5p in non-cancer group and GC of different stages (***, $P < 0.001$). (I-J) ROC curve of miR-223-3p, miR-425-5p and the combined miRNA in distinguishing GC of (I) early stage and (J) late stage from non-cancer group.

Next, miR-223-3p and U6 plasmids with gradient concentrations (from $2 \times 10^7$ fg/μL to $2 \times 10^{-4}$ fg/μL, named S1-S12) were measured by ddPCR and qRT-PCR, respectively. Figure S3A illustrated that the copy number of detected targets gradually decreased with the increase of dilution ratio. The linear range of miR-223-3p was estimated from $2 \times 10^5$ fg/μL to $2 \times 10^{-2}$ fg/μL with a limit of quantitation (LOQ) of 5.39 copies/μL, while U6 achieved a linear range from $2 \times 10^5$ fg/μL to $2 \times 10^{-1}$ fg/μL with a LOQ of 12.25 copies/μL (Fig. 7C-D, Table S4). LOQ was estimated as the lowest concentration in a sample with a coefficient of variation (CV) $\leq$ 25 %. Consequently, ddPCR showed wider detection range and higher sensitivity than qRT-PCR (Figure S3B, C, Table S4). We then evaluated the specificity of ddPCR by detecting plasmids with unmatched primers. Fig. 7E showed that clusters of droplets only obtained when the primer specifically targeted to the plasmids encoding corresponding genes. Overall, these data suggest that ddPCR has improved sensitivity, specificity, and accuracy than qRT-PCR in detecting Neu-Exo miRNAs.

### *3.7. Detection of miRNAs in Neu-Exo for gastric cancer diagnosis by ddPCR*

We next evaluated the diagnostic performance of Neu-Exo miR-223-3p in 34 healthy individuals, 31 BGD patients and 52 GC patients. The ratio of absolute copy number of miR-223-3p to U6 was defined as the relative expression level of miR-223-3p (Figure S3D). As shown in Fig. 7F, the relative expression level of Neu-Exo miR-223-3p was significantly increased in GC group compared to HC and BGD groups. In addition, Neu-Exo miR-223-3p presented gradually increased expression in GC patients with different stages and showed a higher expression in early stage GC patients than non-cancer subjects (Fig. 7G). Pearson correlation analysis showed that the miR-223-3p expression level detected by ddPCR was highly associated with that measured by qRT-PCR ($r = 0.610$, $P < 0.0001$) (Figure S3E). As illustrated in Fig. 7H and Table S5, ROC analysis indicated that the AUC of Neu-Exo miR-223-3p was 0.929 to distinguish GC patients from healthy controls, and 0.926 to differentiate between BGD and GC groups. Moreover, Neu-Exo miR-223-3p showed high differential performance in non-cancer groups and GC of different stages (AUC of 0.930 for early stage, AUC of 0.927 for late stage). In summary, compared to qRT-PCR, ddPCR performed

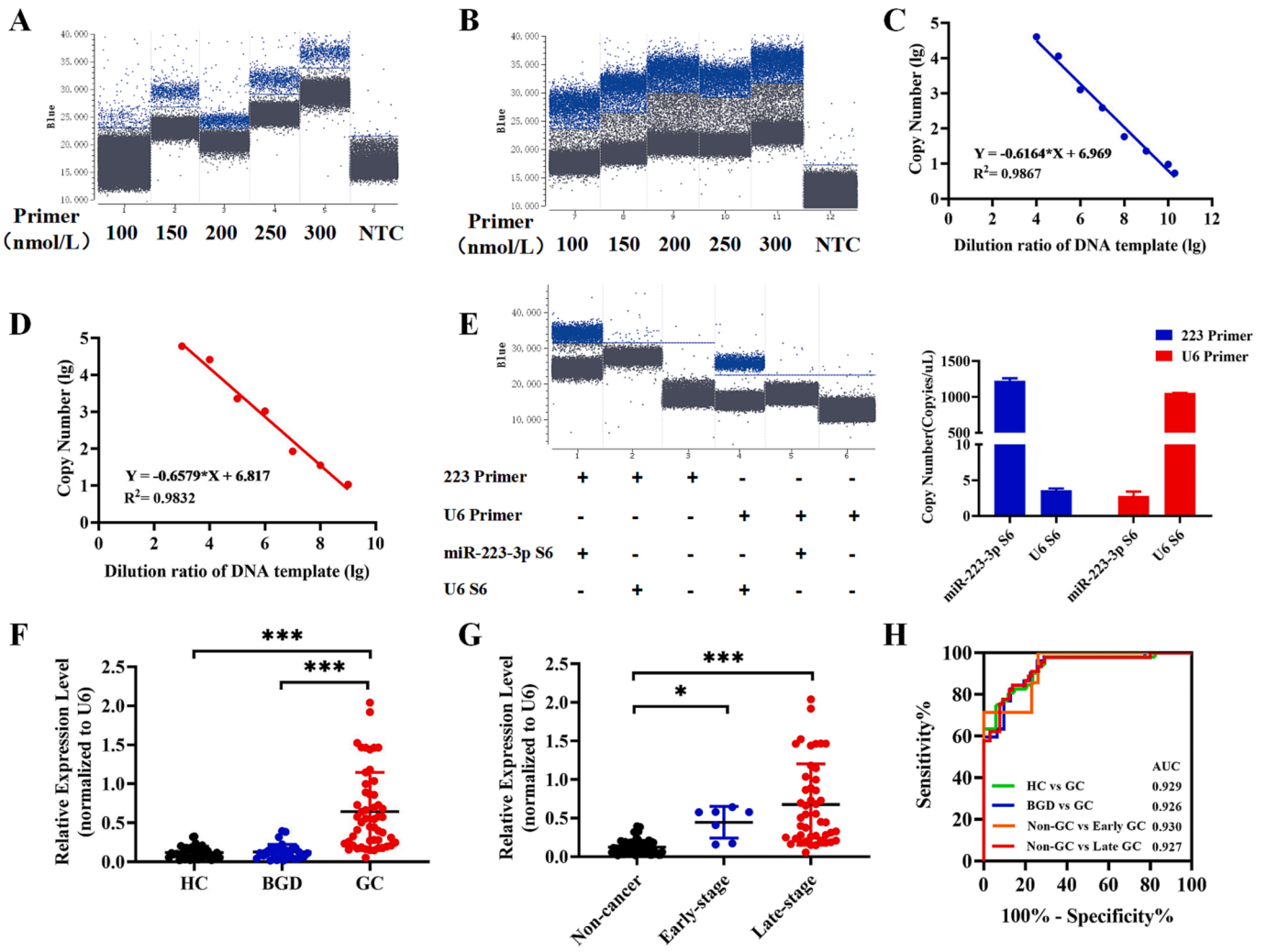


**Fig. 7.** MiRNA detection by ddPCR and the diagnostic efficiency in gastric cancer. (A-B) Optimization of primer concentration for (A) miR-223-3p and (B) U6. (C-D) Linear curve of the copy number of detected targets and plasmids with gradient dilutions for (C) miR-223-3p and (D) U6. (E) Specificity assay of ddPCR by detecting with unmatched primers. (F-G) The relative expression of Neu-Exo-derived miR-223-3p in (F) HC, BGD and GC groups (G) non-cancer group and GC of different stages (***, $P < 0.001$). (H) ROC curve of miR-223-3p in distinguishing between GC patients, BGD patients and healthy controls, and also GC of different stages.

more sensitive detection of Neu-Exo miRNA and higher diagnostic efficiency of GC.

## 4. Discussion

In this study, we explored the value of Neu-Exo miRNAs as accurate biomarkers in gastric cancer diagnosis. Anti-CD66b antibody-coupled Dynabeads were developed for Neu-Exo separation and a dual antibody-assisted fluorescent Dynabeads method was established to detect the abundance of $CD66b^+$ Neu-Exo, which showed significant discrimination between GC patients and healthy individuals. RNA sequencing identified that miR-223-3p was highly expressed in Neu-Exo and had a high diagnostic value in gastric cancer. In addition, ddPCR detection further improved the performance of miR-223-3p in $CD66b^+$ Neu-Exo for early and differential diagnosis of gastric cancer. These findings suggest the potential of Neu-Exo in gastric cancer diagnosis, which may shed light on liquid biopsy for cancer at the early stage.

Currently, immune cell-derived exosomes are demonstrated to be involved in tumor development and may be biomarkers for cancer diagnosis and therapy [23,24]. Neutrophils are the most abundant cells in human peripheral blood and play important roles in tumor progression [11]. In this study, we explored the clinical significance of Neu-Exo and their derived miRNAs in gastric cancer liquid biopsy. The antibody against neutrophil-specific protein CD66b was coupled with Dynabeads for Neu-Exo separation, and obtained an increased enrichment of exosomes (>80 %) than previous studies [25–27]. Compared to other exosome separation platforms such as $Fe_3O_4$ magnetic beads and microfluidic chips [21,28], the Dynabeads method exhibits the advantages of low price, superparamagnetic properties and no complicated fabrication. In addition, a dual antibody-assisted fluorescent Dynabeads method was developed to detect the abundance of serum $CD66b^+$ Neu-Exo, which simplifies the procedures for nanoscale particle detection and achieves sensitive detection of exosomes by common flow cytometry. We found that the concentration of $CD66b^+$ Neu-Exo was significantly upregulated in the serum of GC patients and could be used as a promising biomarker for gastric cancer diagnosis.

Meanwhile, we explored the miRNA profile of serum Neu-Exo to investigate the value of their derived miRNAs in gastric cancer diagnosis. MiR-223-3p was found enriched in serum Neu-Exo and elevated in GC patients compared to benign gastric disease patients and healthy controls. Previous studies indicate that miR-223 modulates the malignancy of cancer cells via distinct mechanisms [29]. Exosome-derived miR-223 is associated with tumor progression, metastasis and drug resistance, and may be potential biomarker for cancer diagnosis and prognosis [30]. Hence, we compared the expression level of miRNA in total Serum-Exo and Neu-Exo. MiR-223-3p was upregulated in gastric

cancer patients both in matched Serum-Exo and Neu-Exo. However, ROC curve indicated that compared to Serum-Exo, Neu-Exo miR-223-3p could better distinguish between GC and BGD, GC and HC groups (AUC $> 0.8$). Moreover, Neu-Exo showed better performance in the differentiation between different stages of GC group and non-cancer group (AUC $> 0.8$). In addition, the expression level of Neu-Exo miR-223-3p was significantly correlated with distant metastasis of gastric cancer. Therefore, miR-223-3p of Neu-Exo achieved a superior diagnostic efficiency than that of total Serum-Exo, suggesting that the analysis of Neu-Exo subsets may reveal the unique molecular profile of neutrophils and address the challenge of exosome heterogeneity in current studies.

Nowadays, droplet digital PCR has been widely applied to detect rare sequences due to the advantages of outstanding sensitivity, high specificity and accuracy [31]. Hence, we used ddPCR to detect the relative expression level of Neu-Exo miR-223-3p. The optimization of primer concentrations significantly improved the dispersion of droplet clusters. Linear range curves indicated that compared to qRT-PCR, ddPCR obtained a wider detection range and lower detection sensitivity, suggesting that ddPCR is more suitable for the detection of low abundance molecules and early diagnosis of gastric cancer. Moreover, compared with qRT-PCR, ddPCR exhibited higher diagnostic efficiency to distinguish GC patients from BGD and HC groups (AUC $> 0.9$), as well as different stages of GC group from non-cancer group (AUC $> 0.9$). Therefore, ddPCR shows better detection efficiency than qRT-PCR. We expect that sensitive and specific exosomal biomarkers combined with highly-efficient detection methods could provide a new prospect for cancer liquid biopsy.

## 5. Conclusion

In summary, we explored the value of Neu-Exo in gastric cancer diagnosis. Dynabeads-based separation system achieved highly efficient separation and recovery of Neu-Exo. Dual antibody-assisted fluorescent Dynabeads enabled sensitive detection of Neu-Exo by simple flow cytometry analysis. Through RNA sequencing, candidate miRNA biomarkers from Neu-Exo were identified and validated in clinical samples. The application of ddPCR further improved the diagnostic efficiency of Neu-Exo miRNAs in gastric cancer. Therefore, we expect that Neu-Exo miRNAs may serve as novel and accurate biomarkers for gastric cancer diagnosis, and ddPCR could provide a promising tool for their detection.

## Funding

This work was supported by the National Natural Science Foundation of China (82372909, 81972310), the Distinguished Young Scholar Project of Jiangsu Province (BK20200043), the Key Laboratory of Molecular Diagnostics and Precision Medicine for Surgical Oncology in Gansu Province (2019GSZDSYS01, 2019GSZDSYS02), the Non-profit Central Research Institute Fund of Chinese Academy of Medical Sciences (NLDTG2020002), Priority Academic Program Development of Jiangsu Higher Education Institutions (PAPD), Nantong Science and Technology Bureau Project (JC2021092), Postgraduate Research & Practice Innovation Program of Jiangsu Province (KYCX21_3405, KYCX22_3713).

## CRediT authorship contribution statement

**Dan Yu:** Data curation, Methodology, Visualization, Writing – original draft. **Jiahui Zhang:** Investigation, Validation. **Maoye Wang:** Software, Validation. **Runbi Ji:** Methodology. **Hui Qian:** Resources, Supervision. **Wenrong Xu:** Resources, Supervision. **Hongbo Zhang:** Resources, Supervision. **Jianmei Gu:** Resources, Supervision. **Xu Zhang:** Funding acquisition, Project administration, Supervision, Writing – review & editing.

## Declaration of competing interest

The authors declare that they have no known competing financial interests or personal relationships that could have appeared to influence the work reported in this paper.

## Data availability

Data will be made available on request.

## Appendix A. Supplementary data

Supplementary data to this article can be found online at https://doi.org/10.1016/j.cca.2024.117773.

## References

[1] E.C. Smyth, M. Nilsson, H.I. Grabsch, N.C. van Grieken, F. Lordick, Gastric cancer, Lancet 396 (2020) 635–648, https://doi.org/10.1016/S0140-6736(20)31288-5.
[2] R. Kalluri, V.S. LeBleu, The biology function and biomedical applications of exosomes, Science 367 (2020) eaau6977, https://doi.org/10.1126/science.aau6977.
[3] H. Di, Z. Mi, Y. Sun, X. Liu, X. Liu, A. Li, Y. Jiang, H. Gao, P. Rong, D. Liu, Nanozyme-assisted sensitive profiling of exosomal proteins for rapid cancer diagnosis, Theranostics 10 (2020) 9303–9314, https://doi.org/10.7150/thno.46568.
[4] N. Sun, Y.T. Lee, R.Y. Zhang, R. Kao, P.C. Teng, Y. Yang, P. Yang, J.J. Wang, M. Smalley, P.J. Chen, M. Kim, S.J. Chou, L. Bao, J. Wang, X. Zhang, D. Qi, J. Palomique, N. Nissen, S.H.B. Han, S. Sadeghi, R.S. Finn, S. Saab, R.W. Busuttil, D. Markovic, D. Elashoff, H.H. Yu, H. Li, A.P. Heaney, E. Posadas, S. You, J. D. Yang, R. Pei, V.G. Agopian, H.R. Tseng, Y. Zhu, Purification of HCC-specific extracellular vesicles on nanosubstrates for early HCC detection by digital scoring, Nat. Commun. 11 (2020) 4489, https://doi.org/10.1038/s41467-020-18311-0.
[5] S.A. Melo, L.B. Luecke, C. Kahlert, A.F. Fernandez, S.T. Gammon, J. Kaye, V. S. LeBleu, E.A. Mittendorf, J. Weitz, N. Rahbari, C. Reissfelder, C. Pilarsky, M. F. Fraga, D. Piwnica-Worms, R. Kalluri, Glypican-1 identifies cancer exosomes and detects early pancreatic cancer, Nature 523 (2015) 177–182, https://doi.org/10.1038/nature14581.
[6] S. Tian, Y. Chu, J. Hu, X. Ding, Z. Liu, D. Fu, Y. Yuan, Y. Deng, G. Wang, L. Wang, Z. Wang, Tumour-associated neutrophils secrete AGR2 to promote colorectal cancer metastasis via its receptor CD98hc-xCT, Gut 71 (2022) 2489–2501, https://doi.org/10.1136/gutjnl-2021-325137.
[7] G. Bellomo, C. Rainer, V. Quaranta, Y. Astuti, M. Raymant, E. Boyd, R. Stafferton, F. Campbell, P. Ghaneh, C.M. Halloran, D.E. Hammond, J.P. Morton, D. Palmer, D. Vimalachandran, R. Jones, A. Mielgo, M.C. Schmid, Chemotherapy-induced infiltration of neutrophils promotes pancreatic cancer metastasis via Gas6/AXL signalling axis, Gut 71 (2022) 2284–2299, https://doi.org/10.1136/gutjnl-2021-325272.
[8] L. Yang, Q. Liu, X. Zhang, X. Liu, B. Zhou, J. Chen, D. Huang, J. Li, H. Li, F. Chen, J. Liu, Y. Xing, X. Chen, S. Su, E. Song, DNA of neutrophil extracellular traps promotes cancer metastasis via CCDC25, Nature 583 (2020) 133–138, https://doi.org/10.1038/s41586-020-2394-6.
[9] M. Perego, V.A. Tyurin, Y.Y. Tyurina, J. Yellets, T. Nacarelli, C. Lin, Y. Nefedova, A. Kossenkov, Q. Liu, S. Sreedhar, H. Pass, J. Roth, T. Vogl, D. Feldser, R. Zhang, V. E. Kagan, D.I. Gabrilovich, Reactivation of dormant tumor cells by modified lipids derived from stress-activated neutrophils, Sci. Transl. Med. 12 (2020) eabb5817, https://doi.org/10.1126/scitranslmed.abb5817.
[10] M.E. Shaul, Z.G. Fridlender, Tumour-associated neutrophils in patients with cancer, Nat. Rev. Clin. Oncol. 16 (2019) 601–620, https://doi.org/10.1038/s41571-019-0222-4.
[11] C.C. Hedrick, I. Malanchi, Neutrophils in cancer: heterogeneous and multifaceted, Nat. Rev. Immunol. 22 (2022) 173–187, https://doi.org/10.1038/s41577-021-00571-6.
[12] T.J. Li, Y.M. Jiang, Y.F. Hu, L. Huang, J. Yu, L.Y. Zhao, H.J. Deng, T.Y. Mou, H. Liu, Y. Yang, Q. Zhang, G.X. Li, Interleukin-17-producing neutrophils link inflammatory stimuli to disease progression by promoting angiogenesis in gastric cancer, Clin. Cancer Res. 23 (2017) 1575–1585, https://doi.org/10.1158/1078-0432.CCR-16-0617.
[13] S. Li, S. Sun, H. Sun, P. Ma, J. Zhang, Y. Cao, C. Liu, X. Zhang, W. Wang, Z. Li, Y. Ma, Y. Xue, Y. Zhao, A risk signature with inflammatory and immune cells infiltration predicts survival and efficiency of chemotherapy in gastric cancer, Int. Immunopharmacol. 96 (2021) 107589, https://doi.org/10.1016/j.intimp.2021.107589.
[14] X.Y. Zhang, Z.C. Chen, N. Li, Z.H. Wang, Y.L. Guo, C.J. Tian, D.J. Cheng, X.Y. Tang, L.X. Zhang, Exosomal transfer of activated neutrophil-derived lncRNA CRNDE promotes proliferation and migration of airway smooth muscle cells in asthma, Hum. Mol. Genet. 31 (2022) 638–650, https://doi.org/10.1093/hmg/ddab283.
[15] A. Tyagi, S.Y. Wu, S. Sharma, K. Wu, D. Zhao, R. Deshpande, R. Singh, W. Li, U. Topaloglu, J. Ruiz, K. Watabe, Exosomal miR-4466 from nicotine-activated neutrophils promotes tumor cell stemness and metabolism in lung cancer

metastasis, Oncogene 41 (2022) 3079–3092, https://doi.org/10.1038/s41388-022-02322-w.
[16] J. Wang, X. Wang, Y. Guo, L. Ye, D. Li, A. Hu, S. Cai, B. Yuan, S. Jin, Y. Zhou, Q. Li, L. Zheng, Q. Tong, Therapeutic targeting of SPIB/SPI1-facilitated interplay of cancer cells and neutrophils inhibits aerobic glycolysis and cancer progression, Clin. Transl. Med. 11 (2021) e588.
[17] S.L. Shu, Y. Yang, C.L. Allen, E. Hurley, K.H. Tung, H. Minderman, Y. Wu, M. S. Ernstoff, Purity and yield of melanoma exosomes are dependent on isolation method, J. Extracell. Vesicles. 9 (2020) 1692401, https://doi.org/10.1080/20013078.2019.1692401.
[18] J. Lim, B. Kang, H.Y. Son, B. Mun, Y.-M. Huh, H.W. Rho, T. Kang, J. Moon, J.-J. Lee, S.B. Seo, S. Jang, S.U. Son, J. Jung, S. Haam, E.-K. Lim, Microfluidic device for one-step detection of breast cancer-derived exosomal mRNA in blood using signal-amplifiable 3D nanostructure, Biosens. Bioelectron. 197 (2022) 113753, https://doi.org/10.1016/j.bios.2021.113753.
[19] M. Huang, J. Yang, T. Wang, J. Song, J. Xia, L. Wu, W. Wang, Q. Wu, Z. Zhu, Y. Song, C. Yang, Homogeneous, Low-volume, Efficient, and Sensitive Quantitation of Circulating Exosomal PD-L1 for Cancer Diagnosis and Immunotherapy Response Prediction, Angew. Chem. Int. Ed. Engl. 59 (2020) 4800–4805, https://doi.org/10.1002/anie.201916039.
[20] A. Bonifay, S. Robert, B. Champagne, P.-R. Petit, A. Eugène, C. Chareyre, A.-C. Duchez, M. Vélier, S. Fritz, L. Vallier, R. Lacroix, F. Dignat-George, A new strategy to count and sort neutrophil-derived extracellular vesicles: Validation in infectious disorders, J. Extracell. Vesicles 11 (2022) e12204.
[21] J. Chen, Y. Xu, Y. Lu, W. Xing, Isolation and visible detection of tumor-derived exosomes from plasma, Anal. Chem. 90 (2018) 14207–14215, https://doi.org/10.1021/acs.analchem.8b03031.
[22] S. Cho, H.C. Yang, W.J. Rhee, Simultaneous multiplexed detection of exosomal microRNAs and surface proteins for prostate cancer diagnosis, Biosens. Bioelectron. 146 (2019) 111749, https://doi.org/10.1016/j.bios.2019.111749.
[23] J. Lan, L. Sun, F. Xu, L. Liu, F. Hu, D. Song, Z. Hou, W. Wu, X. Luo, J. Wang, X. Yuan, J. Hu, G. Wang, M2 macrophage-derived exosomes promote cell migration and invasion in colon cancer, Cancer Res. 79 (2019) 146–158, https://doi.org/10.1158/0008-5472.CAN-18-0014.
[24] S.G. Dosil, S. Lopez Cobo, A. Rodriguez Galan, I. Fernandez Delgado, M. Ramirez Huesca, P. Milan Rois, M. Castellanos, A. Somoza, M.J. Gómez, H.T. Reyburn, M. Vales Gomez, F. Sánchez Madrid, L. Fernandez Messina, Natural killer (NK) cell-derived extracellular-vesicle shuttled microRNAs control T cell responses, Elife 11 (2022) e76319.
[25] Y. Zhang, X. Tong, L. Yang, R. Yin, K.J.S. Deng, A.B. Chemical, A herringbone mixer based microfluidic device HBEXO-chip for purifying tumor-derived exosomes and establishing miRNA signature in pancreatic cancer, Sensor. Actuat. B Chem. 332 (2021) 129511, https://doi.org/10.1016/j.snb.2021.129511.
[26] S. Cai, B. Luo, P. Jiang, X. Zhou, F. Lan, Q. Yi, Y. Wu, Immuno-modified superparamagnetic nanoparticles via host-guest interactions for high-purity capture and mild release of exosomes, Nanoscale 10 (2018) 14280–14289, https://doi.org/10.1039/c8nr02871k.
[27] C.Y. Sung, C.C. Huang, Y.S. Chen, K.F. Hsu, G.B. Lee, Isolation and quantification of extracellular vesicle-encapsulated microRNA on an integrated microfluidic platform, Lab Chip 21 (2021) 4660–4671, https://doi.org/10.1039/d1lc00663k.
[28] Y. Lu, L. Ye, X. Jian, D. Yang, H. Zhang, Z. Tong, Z. Wu, N. Shi, Y. Han, H. Mao, Integrated microfluidic system for isolating exosome and analyzing protein marker PD-L1, Biosens. Bioelectron. 204 (2022) 113879, https://doi.org/10.1016/j.bios.2021.113879.
[29] J. Jeffries, W. Zhou, A.Y. Hsu, Q. Deng, miRNA-223 at the crossroads of inflammation and cancer, Cancer Lett. 451 (2019) 136–141, https://doi.org/10.1016/j.canlet.2019.02.051.
[30] X. Zhu, H. Shen, X. Yin, M. Yang, H. Wei, Q. Chen, F. Feng, Y. Liu, W. Xu, Y. Li, Macrophages derived exosomes deliver miR-223 to epithelial ovarian cancer cells to elicit a chemoresistant phenotype, J. Exp. Clin. Cancer Res. 38 (2019) 81, https://doi.org/10.1186/s13046-019-1095-1.
[31] C. Liu, B. Li, H. Lin, C. Yang, J. Guo, B. Cui, W. Pan, J. Feng, T. Luo, F. Chu, X. Xu, L. Zheng, S. Yao, Multiplexed analysis of small extracellular vesicle-derived mRNAs by droplet digital PCR and machine learning improves breast cancer diagnosis, Biosens. Bioelectron. 194 (2021) 113615, https://doi.org/10.1016/j.bios.2021.113615.